Lab on a Chip

Accepted Manuscript

ROYAL SOCIETY OF CHEMISTRY

www.rsc.org/loc

Lab on a Chip

RSCPublishing

ARTICLE

Microfluidic serpentine antennas with designed mechanical tunability

Cite this: DOI: 10.1039/xoxxoooooox

YongAn Huang*, Yezhou Wang, Lin Xiao, Huimin Liu, Wentao Dong, Zhouping Yin*

Received ooth June 2014,
Accepted ooth July 2014

DOI: 10.1039/xoxxoooooox

www.rsc.org/loc

This paper describes the design and characterization of microfluidic serpentine antennas with reversible stretchability and designed mechanical frequency modulation (FM). The microfluidic antennas are designed based on the Possion's ratio of the elastomer in which the liquid alloy antenna is embedded, to controllably decrease, stabilize or increase its resonance frequency when being stretched. Finite element modelling was used in combination with experimental verification to investigate the effects of substrate dimensions and antenna aspect ratios for the FM sensitivity to uniaxial stretching. It could be designed within the range of -1.2 to 0.6 GHz/100%. When the aspect ratio of the serpentine antenna is between 1.0 and 1.5, the resonance frequency is stable under stretching, bending, and twisting. The presented microfluidic serpentine antenna design could be utilized in wireless mobile communication modules of wearable electronics, with a stable resonance frequency under dynamic applied strain up to 50%.

1 Introduction

"Stretchability" in electronics has the potential to open up for new opportunities, particularly for large-area wearable devices that can conform to a curved surface or to bending, twisting and stretching while in use with movable parts [1-6]. Stretchable antennas offer attractive applications such as reconfigurable antennas [7], large-area wireless sensors [8], wireless recharging systems [9], RF communication [10], and mechanically tuneable antenna [11]. Stretchable antennas are commonly built by three methods: transfer printing of metal film antennas [10, 12], soft nanolithography of microfluidic antennas [13-16], or direct printing liquid alloy antennas [17-19]. The serpentine metal antennas presented may commonly stabilize the frequency, but they cannot avoid out-of-surface wrinkling and realize mechanical frequency modulation (FM). Two unbalanced loop antennas and a half-wave dipole antenna have been reported to be fabricated by injecting Galinstan (Ga 68.5%, In 21.5%, and Sn 10%) and EGaIn (eutectic gallium indium alloy, Ga 75.5% and In 24.5%) into microfluidic channels in elastic PDMS substrates [11, 13, 14]. The existing microfluidic antennas are reversibly deformable and mechanically tuneable, but their resonance frequency always monotonously decreases under stretching. Also, they are unable to stabilize the resonance frequency under stretching, and their mechanical FM sensitivity (the sensitivity of resonance frequency to applied strain) is fixed to each type of antenna. It hinders applications which need a stable resonance frequency in expansion and shrinkage. Further, it could also be interesting to utilize that the resonance frequency can be designed to increase when being stretched. In conclusion, it is important to enable a simple and versatile design that can allow for mechanically adaptive antennas to decrease, stabilize or increase their resonance frequency under stretching.

This paper describes a novel technique to design stretchable, mechanically tuneable microfluidic antennas that can work in the status of overclocking, at constant frequency or underclocking under stretching. The antennas consist of a liquid alloy, which is able to fill the designed microchannels rapidly at room temperature and possesses a thin oxide ''skin'' that keeps it mechanically stable [11, 20]. Microstructured serpentine channels with various aspect ratios are designed and embedded in an elastic Ecoflex substrate to realize FM with a designed mechanical sensitivity. This omits the limitation of existing stretchable antennas, all having a built-in mechanical tunability that cannot be changed.

2 Principles and Implementation

Todays' mechanically tuneable microfluidic antennas hinder the integration of microfluidic antennas in applications that need a stable resonance frequency or a specific tunability under stretching. The serpentine antenna is commonly used to decrease the physical size of an antenna while maintaining its electrical length and the antenna is not stretchable.

Here we design serpentine microchannels embedded in an Ecoflex substrate, to fabricate microfluidic stretchable antennas. Figure 1 shows the basic design of the stretchable serpentine antennas, where the Poisson effect is used to control the antenna length when it is stretched. The large Poisson ratio of Ecoflex ($v_{Ecoflex}$=0.49) will make the substrate shrink significantly in the perpendicular direction to the direction it is stretched. The shape of the microfluidic antennas is defined by the serpentine microchannels in Ecoflex substrate. As a proof of concept, we designed and fabricated a half-wave dipole antenna. The dipole antenna consisted of two symmetric branches separated by a small gap. Each antenna branch is saddle-shaped, comprising of semicircle and straight segments. The important design parameters include $h_{antenna}$, $w_{antenna}$, $h_{substrate}$ and $w_{substrate}$. The $h_{antenna}$ and $w_{antenna}$ can completely determine the shape of the serpentine antennas. The core of design is to determine the aspect ratio $\alpha=h_{antenna}/w_{antenna}$, to adjust the change of length of the serpentine antennas during large elongation of substrate, to mechanically tune (decrease, stabilize and increase) the resonance frequency.

The antenna length was chosen to give a resonance frequency around 1.6 GHz; and the width and thickness were then chosen to yield reasonably low electrical resistance (<0.1Ω) benefitting from EGaIn's low electrical resistivity (29.4×10^{-6}Ω-cm). Each antenna branch has dimensions of 32 *mm* (length) × 0.5 *mm* (width) × 0.5 *mm* (thickness) when being unstrained, and the gap is 2 mm. The ability of the liquid metal to flow during deformation of the Ecoflex ensures electrical continuity. The Ecoflex substrate is $h_{substrate}$ =40 *mm* and $w_{substrate}$ =70 *mm*.

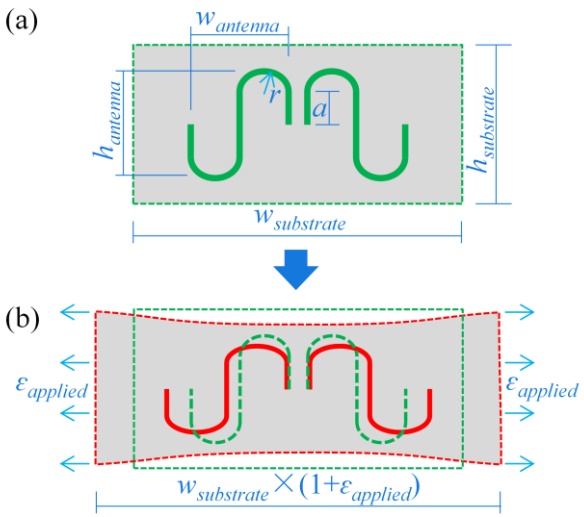

Figure 1 The design principle and the serpentine microfluidic antenna: a) the initial serpentine antenna, and b) the strained serpentine antenna.

In order to guarantee RF communication, the resonance frequency should be stabilized even when the antennas are stretched in inflatable devices. The serpentine antennas can keep the length constant when stretched largely. After stretched, the antennas change from the initial length $l_0 = 4a + 2\pi r$ to $l_{stretched} = 4\left(\frac{h_{antenna}}{2} - r\right)\left(1 - \frac{\varepsilon_{applied}}{2}\right) + \pi r\left(3 + \frac{3\varepsilon_{applied}}{4} - \sqrt{\left(1-\varepsilon_{applied}\right)\left(1 - \frac{\varepsilon_{applied}}{2}\right)}\right)$. In order to keep the resonance frequency invariable, one can make $l_{stretched}=l_0$ in strain, then can get aspect ratio $\alpha \approx 1.1$, with the assumption of small deformation. Practically, the aspect ratio α is related with the applied strain. The critical aspect ratios, to divide the three kinds of frequency modulating modes, are validated by finite element analysis and by experiments. The commercial software, ANSYS, is adopted, and the element Solid185 and Fluid80 denote Ecoflex and liquid metal respectively. Mooney-Rivlin model of hyperelastic material is used to simulate the Ecoflex substrate. Young's modulus is $E_{Ecoflex}$=60*kPa*, and Possion ratio is $v_{Ecoflex}$=0.49, then one can get the parameters in Mooney-Rivlin model: $C_{10} = \frac{E_{Ecoflex}}{5\left(1+v_{Ecoflex}\right)}$, $C_{01} = \frac{1}{4}C_{10}$, and $D = \frac{6\left(1-2v_{Ecoflex}\right)}{E_{Ecoflex}}$. Figure 2 shows that the serpentine microchannels with α=1.1~1.4 usually elongate less than 2%, even when the applied strain reaches 50%. The experiment data are close to the simulation data and the fitted curves. It means that the resonance frequency can keep invariable even when the whole microfluidic antenna is stretched up to more than 50%. The antennas can repeatedly withstand complex mechanical deformation and return to their original state after removal of the applied strain, while retaining a high efficiency (> 95 %) in radiation.

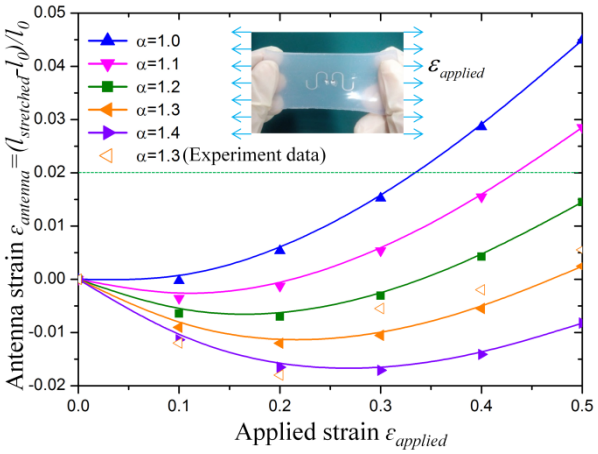

Figure 2 The change of antenna length compared to the applied strain. The solid dots are simulation data, the curves are their fitted results, and the hollow triangles are the experiment data.

3 Materials and Experiments

Figure 3a describes the fabrication of serpentine microfluidic antennas. We used Ecoflex (up to 1000% strecthability) for the elastic insulating channels that held the antenna branches. The process is based on soft lithography: 1) preparing Ecoflex solution with the crosslinker and prepolymer at a ratio of 1:1 (type 0030, Reynolds Advanced Materials); 2) casting the freshly Ecoflex solution into prepared smooth/patterned mould; 3) peeling the Ecoflex substrate (~2mm thickness) away from the patterned mould and bonding it onto another half-cured Ecoflex substrate to form microstructured channel; 4) curing the composite structure to ensure good bonding at the interface; 5) injecting EGaIn (75% gallium and 25% indium, melting point=15.7℃) through positive pressure, and sealing the EGaIn-filled microfluidic channels with epoxy resin. The liquid metal can be injected into the structured microchannels without heating [21].

Figure 3c-e show that the serpentine antennas can be twisted, bended and stretched. The characteristics of straight antennas and serpentine antennas are compared under strain. We measured the reversible stretchability and resonance frequency of the microfluidic antennas, to demonstrate the mechanical adaptivity of frequency modulation under large strain. The ratio between the reflected and incident power is measured as a function of tensile strain using a vector network analyzer (Agilent E5071C). Three detail properties of antennas are characterized: i) the variation of resonance frequency under large applied strains to show the mechanical tunability with designed FM sensitivity; ii) the return loss to show the increasingly high efficiency of radiation under large applied strains; iii) reversible stretchability with the designable resonance frequency after repetitively stretching the antenna up to a strain of 50 %.

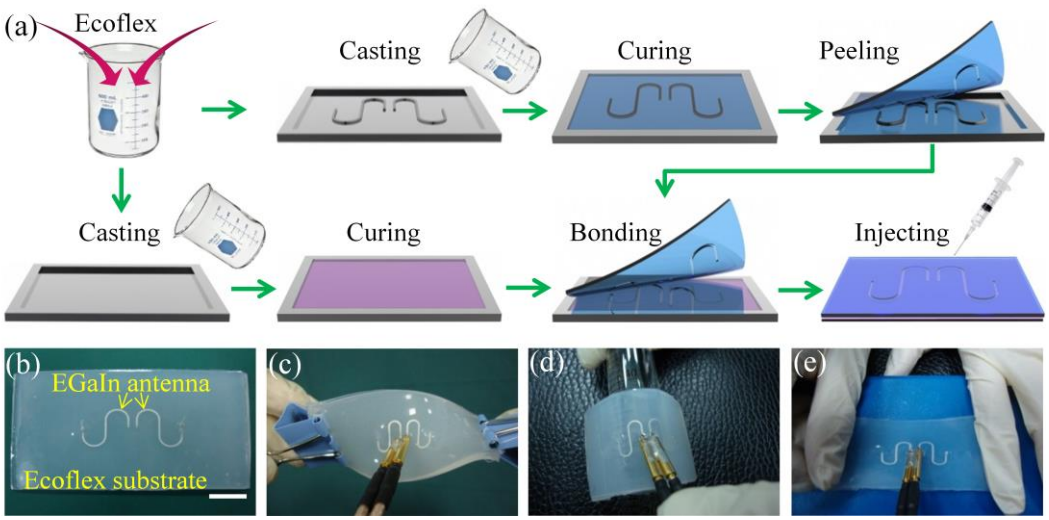

Figure 3 Schematic illustrations and optical micrograph of the stretchable microfluidic antenna: a) the fabrication process of microfluidic antenna; b) the design parameters of the serpentine microfluidic antenna; and c-e) the half-wave dipole antennas are twisted, bended and stretched.

4 Results and Discussion

Figure 4 illustrates the resonance frequency of the straight antenna and serpentine antennas with various aspect ratios changing with gradually increased strain. The applied strain up to 50% is utilized to mechanically tune the length of straight liquid metal antenna, so as to synchronously modulate the resonance frequency from 1.54 to 1.06 GHz. It denotes the extremely negative FM sensitivity of mechanically tuneable antennas, or namely it is the lower limit of envelope diagram of sensitivity. However, the FM sensitivity to applied strain is fixed for the straight microfluidic antenna. Especially the frequency cannot be stabilized at 1.54 GHz, not to mention to the increasing of resonance frequency, when the antennas are stretched. A serpentine microchannel with small aspect ratio, such as $0.5<\alpha<1.0$, will start stepping down the frequency when stretched up to 50%. $\alpha=0.5$ is the minimum ratio for serpentine microchannel. When $1.1<\alpha<1.5$, the resonance frequency keeps stable, and hardly change with the tensile strain. It benefits from the constant length of serpentine antennas even when stretched by the applied strain. When the aspect ratio further increasing (e.g. $\alpha>2$), the resonance frequency will increases with the applied strain $\varepsilon_{applied}$, and usually the electrical signals is too weak to measure.

One can observe from experimental data that the resonance frequency of straight microfluidic antennas is different from that of serpentine one with the same length. At the length of 32 mm, the former is about 1.54 GHz, but the latter is about 1.76 GHz. The resonance frequency of a half-wave dipole antenna can be calculated by $f = k \times \frac{143}{l_{stretched}} \times \frac{1}{\sqrt{\varepsilon_{eff}}}$, where f is the resonance frequency (MHz), $l_{stretched}$ is the length of stretched antenna (m), and ε_{eff} is the effective dielectric constant of Ecoflex (a combination of the dielectric constants of Ecoflex ($\varepsilon \sim 2.1$) and air ($\varepsilon = 1$)), and k is the correction factor (k=1 for straight antenna, and k=1.12 for serpentine one). The resonance frequency decreases monotonously with the increasing of the antenna length. The resonance frequency of the straight antenna decreased from 1.54 GHz to 1.06 GHz in experiment, and it agrees well with theoretical result from 1.54 GHz to 1.1 GHz as the antenna was stretched from its original length l_0 to $l_{stretched}=1.4l_0$. After releasing the applied strain, the resonance frequency returned from 1.06 GHz to 1.54 GHz.

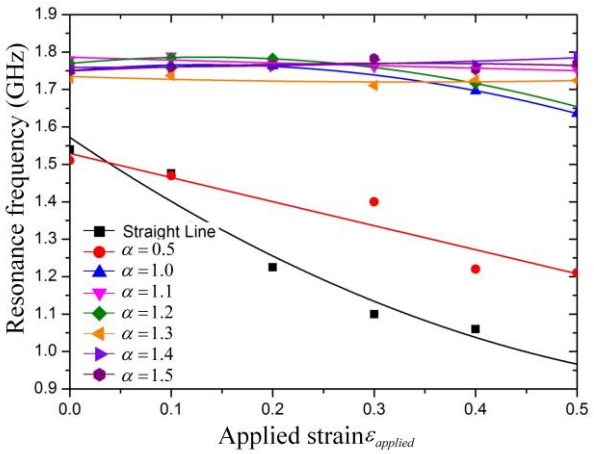

Figure 4 The influence of applied strain on the resonance frequency and antenna strain. The dots are experimental data, and the curves are fitted results.

The return loss $|S_{11}|$ is measured to show the radiation efficiency of the antenna under stretching. If the antenna radiates efficiently, most of the incident power is radiated into free space, and there is little reflected power. This value of reflected power $|S_{11}|$ is -40 dB, −30 dB, −20 dB and −10 dB when 99.99%, 99.9 %, 99 % and 90 % of the input power is radiated from antenna, respectively. Practically, −10 dB indicates enough high efficiency of radiation. For the serpentine antenna with α=1.3, the unstretched antennas exhibited $|S_{11}|$ value of ~−16 dB. As the antenna was stretched, $|S_{11}|$ values varied from ~−23 dB ($\varepsilon_{applied}$=10%) to ~−22.5 dB ($\varepsilon_{applied}$=20%) to ~−29 dB ($\varepsilon_{applied}$=30%) to ~−48 dB ($\varepsilon_{applied}$=40%) to ~−27.5 dB ($\varepsilon_{applied}$=50%), as shown in Figure 5a. It decreases at tensile strain of 50 %, and the main reason may lie in the poor contact between the antennas and test devices. The series of experiments demonstrate that the applied strain plays a positive role in increasing the value of reflected power, namely, the $|S_{11}|$ increases gradually with the applied strain. The serpentine liquid metal antennas become gradually small aspect ratio when the substrate is stretched, and the electrical performance approaches to that of the straight dipole antennas. The serpentine antenna exhibits good radiation efficiency, even when stretched up to 50 %. When stretched further, the length of the antennas will increase slowly with the applied strain, but still far smaller than that of straight one. The reliability is investigated by repeatedly stretching it up to a strain of 50 %, and the antenna exhibited a stable resonance frequency.

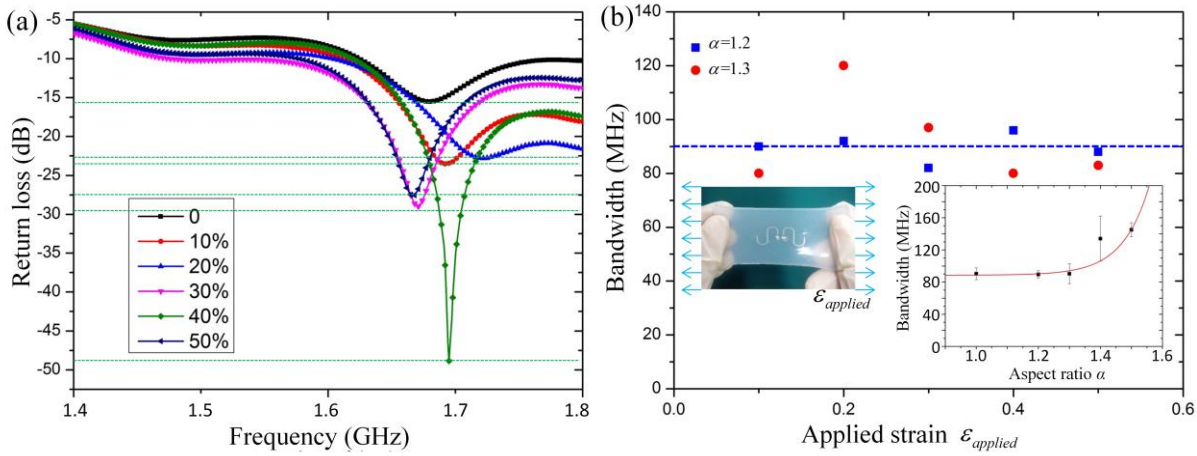

Figure 5 a) The return loss of microfluidic serpentine antenna with aspect ratio α=1.3, related with the applied strain, and b) the bandwidth of microfluidic serpentine antennas depended on the applied strain.

Figure 5b shows that the bandwidth of liquid metal antennas is independent on the applied strain, but dependent on the aspect ratio α in our experiments. In mobile communications system, the VSWR (Voltage Standing Wave Ratio) should be smaller than 1.5:1 (about 14 dB return loss), based on which the bandwidth is defined. The semi-bandwidth is calculated as the frequency difference between at peak and at 14dB. When the antennas are stretched up to 50% with interval of 10%, the measured impedance bandwidth maintains about 90 MHz. Antennas are not often designed for low bandwidth (sharp resonance frequency) in mobile communication. Within the 1.7 GHz band, the proposed antennas show good impedance matching (better than 1.5:1 VSWR). The serpentine antennas almost keep the same bandwidth under stretching. The bandwidth independence of applied strain can effectively emancipate the constraints of antenna design. However, the bandwidth is related with the aspect ratio. The inset shows that the bandwidth is the same when the aspect ratio is between 1.0 and 1.3, and increases when the aspect ratio is larger than 1.4.

Figure 6 illustrates the relationship between the return loss and frequency when the antennas are bent with different radius and twisted with different angle. The serpentine liquid metal antenna with aspect ratio 1.3 is bonded onto three cylinders with different radius. Three radii R=10, 12, 26 *mm* are adopted, and the resonance frequency is very stable. The twist angle can increase the return loss comparable to initial value, and it has little effect on the resonance frequency. This reversible tuning demonstrated the robustness. The microfluidic antennas can undergo repeatedly stretching, without losing its electromagnetic properties. It denotes the curve surface brings very slight influence on the liquid metal antenna, and shows the potential application in conformal electronics and wearable electronics.

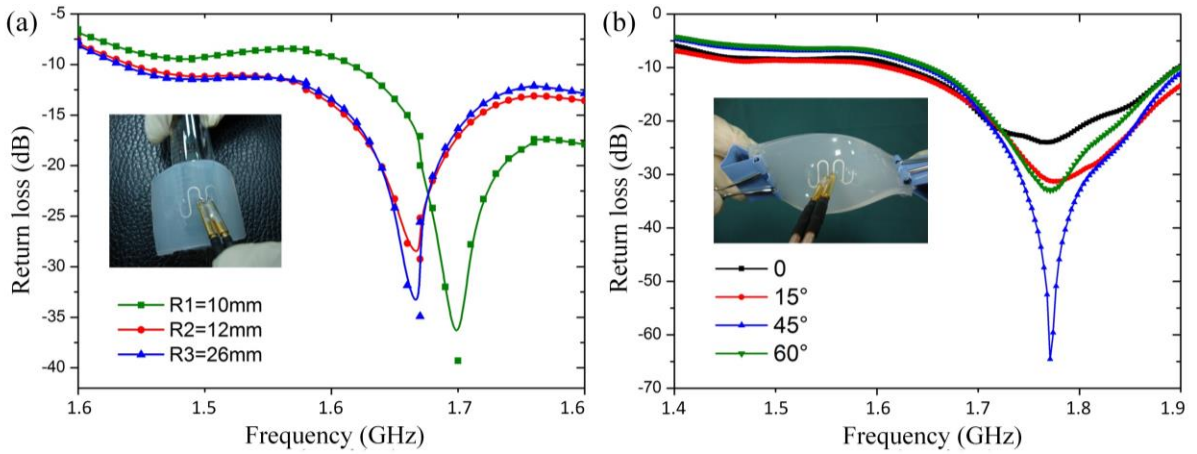

Figure 6 The return loss of serpentine liquid metal antenna with ratio α=1.3, related with: a) various bending radiuses, and b) various twist angles. The substrate is $h_{substrate}$=40*mm* and $w_{substrate}$=70*mm*.

In addition to the antenna shape, the dimension of Ecoflex substrate also plays a very important role in mechanical FM sensitivity. When one clamps the Ecoflex substrate and stretches it along *y*-direction, the Poisson's effect is suppressed due to the small $h_{substrate}$. That is to say the small $h_{substrate}$ prevents the length of microfluidic antenna from contracting during stretching. Figure 7a shows the lateral stretch effect on the resonance frequency of the straight liquid metal antenna embedded in Ecoflex

substrate with $w_{substrate}$=70 *mm* and $h_{substrate}$=40 *mm*. The resonance frequency is strongly influenced by the applied strain $\varepsilon_{applied}$, and the main reason is that $h_{substrate}$ is much smaller than $w_{substrate}$. $h_{substrate}$ is investigated to discover the effect of substrate dimension. Figure 7b shows the physical length reduction of microfluidic antenna with $h_{substrate}$ at the case of applied strain of 10%, 30% and 50%. The results is calculated by finite element simulation (commercial software, ANSYS), and Mooney-Rivlin model of hyperelastic material is used to simulate the Ecoflex substrate. The length is hardly shortened at the case of small $h_{substrate}$, and the reduction becomes larger with the increasing of $h_{substrate}$ and converges when $h_{substrate}$>100 *mm*. It can be proven theoretical and experimentally that lateral reduction converges when the ratio of the length along tensile direction to the length perpendicular to tensile direction is about 1.5. So we design a serpentine microfluidic antenna with $h_{substrate}$=100 *mm* and $w_{substrate}$=70 *mm*, to mechanically tune the frequency with positive FM sensitivity.

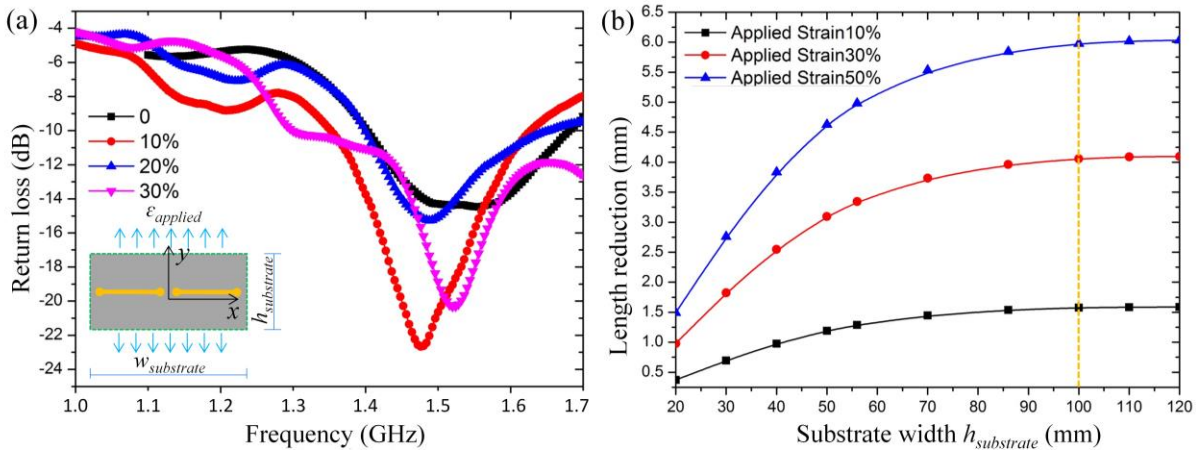

Figure 7 a) The straight liquid metal antenna is stretched along the perpendicular direction, and b) the length reduction of microfluidic antenna related with $h_{substrate}$.

The mechanical adaptivity is to modulate resonance frequency in a programmable manner, rather than merely to decrease the resonance frequency with FM sensitivity like straight microfluidic antennas. It is critical to find the envelope diagram, to determine the range of mechanical FM sensitivity. Based on finite element simulation and experiments, we found the extreme positive and passive sensitivities appear when the straight liquid metal antenna was stretched perpendicular and parallel to antenna, as shown in Figure 8a. The red line denotes the upper limitations that the frequency increases from 1.54 to 1.86 GHz with slope of 0.6 GHz/100%. The black line show the lower limitation that the frequency decreases with slope of -1.2 GHz/100%. All the FM sensitivity is located in the range of envelope diagram. The good agreement between the measurement and theoretical model indicated that the antenna can work as predicted. The direction of applied strain is also critical for microfluidic serpentine antennas. Figure 8b shows two mechanical FMs of the microfluidic serpentine antenna with ratio 1.3 by stretching in two orthogonal directions. The resonance frequency keeps stable when the antenna is stretched along *x*-direction, as the design predicts, and decreases when the antenna is stretched along *y*-direction with FM sensitivity slightly larger than the straight one. One antenna exhibits different capabilities of mechanical FM sensitivity, which is determined by the design and tensile direction.

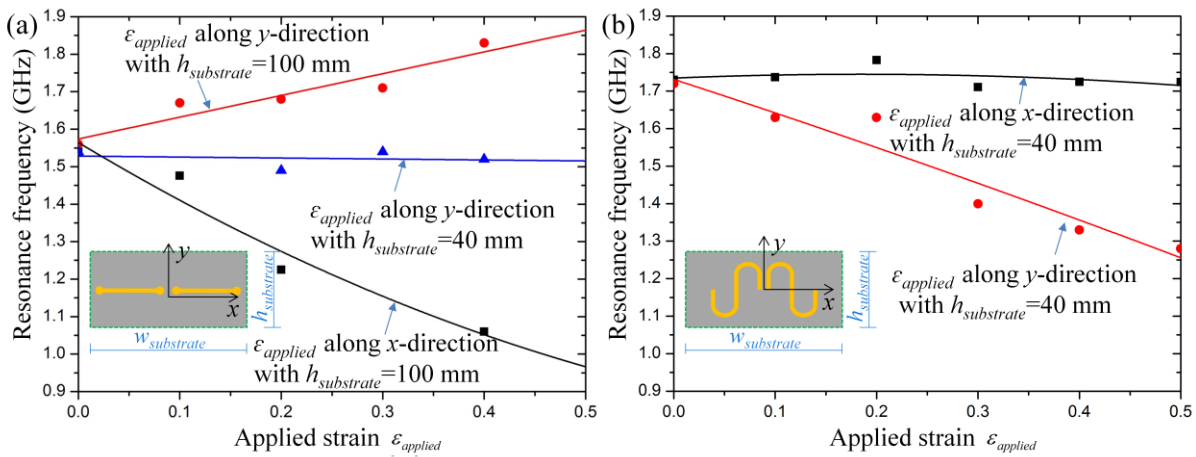

Figure 8 The resonance frequency dependent on the direction of applied strain: a) straight liquid metal antennas, and b) serpentine liquid metal antenna with ratio 1.3. $w_{substrate}$=70*mm*.

The mechanically adaptive microfluidic antenna is designed based on uniaxial tension. In practical applications such as wearable electronics, the substrates stretched bi-axially are inevitable to elongate the antenna length[15], so the antennas are impossible to work in the case of stable frequency or positive FM sensitivity. Here, we presented a strain-isolated design and modular assembly of free-standing antenna sheet. The strain-isolated design is utilized to transform bi-axial tension into uniaxial tension, based on which the presented microfluidic antennas can work in complex working condition. The core is to embed isolation strip in substrate, by use of gap or softer materials (Figure 9a). The microfluidic antennas are merely subjected to tensile strain along the isolation strip. The length of isolation strip determines the isolation effect of bi-axial tension, and the whole strain of antenna decrease monotonously with the strip length, and the results of finite element simulation at the case of applied strain 50% is shown in Figure 9b. When the isolation strips are 125*mm* length with 40*mm* interval, the integrated microfluidic antennas subjected to bi-axial tension is similar with the individual microfluidic antennas with $h_{substrate}$=40 *mm* and $w_{substrate}$=70 *mm* by uniaxial tension (Figure 9c). A modular assembly of microfluidic antenna sheets is encapsulated in an Ecoflex overcoat layer, leading to the production of an integrated antenna array. The free-standing antennas are produced by the peeling-off process [22]. The integrated direction of antenna is selectable, so that the mechanical FM sensitivity can be quickly switched. All the individual sheets can be connected in a reconfigurable manner[23, 24]. Finite element method is adopted to simulate the stretchable device integrated with mechanically adaptive microfluidic antennas. The results show the antenna can work as the design.

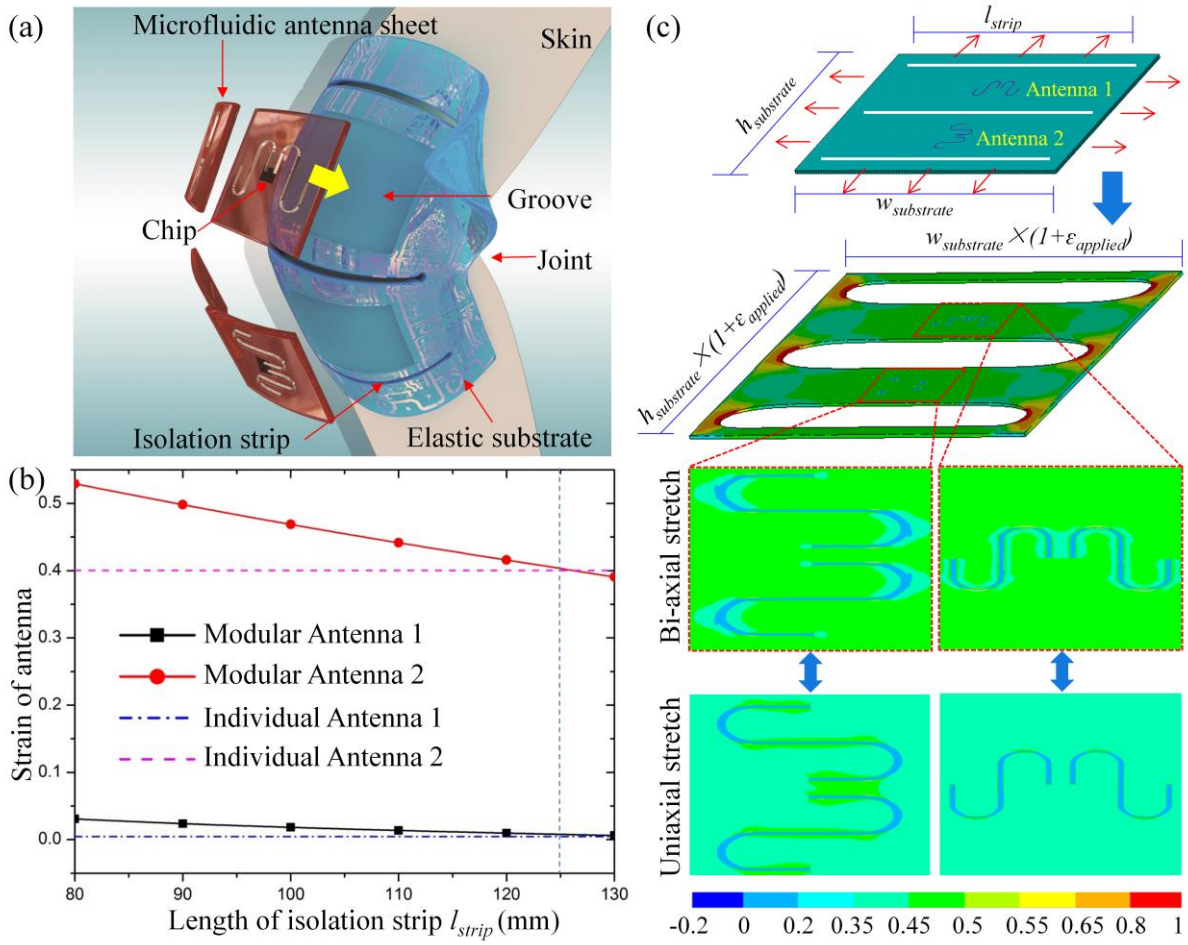

Figure 9 Mechanically adaptive application based on strain-isolated design and modular assembly: a) the integration of microfluidic antenna is based on modular assembly, and the isotopic carrier is designed based on strain-isolated method, b) the influence of strip length on the strain of antenna is given by finite element simulation, and c) the strain simulation of bi-axial stretched modular antenna and uniaxial stretched individual antenna.

Besides the stretchability, the serpentine microfluidic antennas have several additional advantages. i) the resonance frequency can be mechanically modulated by elongating the antenna-substrate system with designed FM sensitivity; ii) the serpentine design can stabilize the resonance frequency, and simultaneously have high stretchability; iii) it can be adopted to incorporate other stretchable 2D and 3D devices thanks to the good performance in status of stretching, bending and twisting; and iv) based on strain-isolated design and modular assembly, it allows the antennas to be easily integrated with other microfluidic components for tuning, sensing, and signal modulation.

4. Summary

The design of microfluidic serpentine antennas is presented for mechanically adaptive frequency modulation. The serpentine channels were fabricated in an Ecoflex matrix and filled it with EGaIn. The stretchable antennas can exhibit mechanical tunability of resonance frequencies, including decreasing, stabilizing, and increasing the resonance frequencies under stretching. It has significant advantages over existing liquid metal antennas, such as designed mechanical FM sensitivity. To the best of our knowledge, this is the first design reported for mechanically adaptive antennas. The antenna can experience complex deformation, including bending, stretching and twisting, meanwhile the resonance frequency is stabilized at the case of applied strain up to 50%. Additionally, the resonance frequency can also increase or decrease in designable manner within the calculated envelope diagram. The antenna preserves its electromagnetic properties after being repeatedly stretched up to a strain of 50 %. The strain-isolated design and modular assembly of individually antenna sheets is presented to address the practical applications. Mechanical compliance of liquid metal antennas may increase the comfort for wearable electronics or implantable medical devices.

Acknowledgments

The authors acknowledge supports from the National Natural Science Foundation of China (51322507, 51175209) and the Fundamental Research Funds for the Central Universities (2013TS019). The general characterization facilities were provided through the Wuhan National Laboratory for Optoelectronics.

Notes and references

* Corresponding author: Y.A. Huang, yahuang@hust.edu.cn, and Z.P. Yin, yinzhp@mail.hust.edu.cn

[a] State Key Laboratory of Digital Manufacturing Equipment and Technology, Huazhong University of Science and Technology, Wuhan, 430074, China. Email: yinzhp@mail.hust.edu.cn

1 D. H. Kim, J. H. Ahn, W. M. Choi, H. S. Kim, T. H. Kim, J. Song, Y. Y. Huang, Z. Liu, C. Lu, J. A. Rogers. *Science*, 2008, **320,** 507-511.
2 T. Sekitani, H. Nakajima, H. Maeda, T. Fukushima, T. Aida, K. Hata, T. Someya. *Nature Mater.*, 2009, **8,** 494-499.
3 Y. Huang, Z. Yin, Y. Xiong. *Thin Solid Films*, 2010, **518,** 1698-1702.
4 Y. A. Huang, Z. P. Yin, Y. L. Xiong. *J. Appl. Mech-T. ASME.*, 2010, **77,** 041016.
5 M. Ramuz, B. C. K. Tee, J. B. H. Tok, Z. Bao. *Adv. Mater.*, 2012, **24,** 3223-3227.
6 Y. Su, J. Wu, Z. Fan, K.-C. Hwang, J. Song, Y. Huang, J. A. Rogers. *J. Mech. Phys. Solids*, 2012, **60,** 487-508.
7 B. A. Cetiner, H. Jafarkhani, J.-Y. Qian, H. J. Yoo, A. Grau, F. De Flaviis. *Communications Magazine, IEEE*, 2004, **42,** 62-70.
8 S. Cheng, Z. G. Wu. *Adv. Funct. Mater.*, 2011, **21,** 2282-2290.
9 S. Xu, Y. Zhang, J. Cho, J. Lee, X. Huang, L. Jia, J. A. Fan, Y. Su, J. Su, H. Zhang, H. Cheng, B. Lu, C. Yu, C. Chuang, T.-i. Kim, T. Song, K. Shigeta, S. Kang, C. Dagdeviren, I. Petrov, P. V. Braun, Y. Huang, U. Paik, J. A. Rogers. *Nat Commun*, 2013, **4,** 1543.
10 D. H. Kim, N. S. Lu, R. Ma, Y. S. Kim, R. H. Kim, S. D. Wang, J. Wu, S. M. Won, H. Tao, A. Islam, K. J. Yu, T. I. Kim, R. Chowdhury, M. Ying, L. Z. Xu, M. Li, H. J. Chung, H. Keum, M. McCormick, P. Liu, Y. W. Zhang, F. G. Omenetto, Y. G. Huang, T. Coleman, J. A. Rogers. *Science*, 2011, **333,** 838-843.
11 J. H. So, J. Thelen, A. Qusba, G. J. Hayes, G. Lazzi, M. D. Dickey. *Adv. Funct. Mater.*, 2009, **19,** 3632-3637.
12 S. Lee, S. Kim, T. T. Kim, Y. Kim, M. Choi, S. H. Lee, J. Y. Kim, B. Min. *Adv. Mater.*, 2012, **24,** 3491-3497.
13 S. Cheng, A. Rydberg, K. Hjort, Z. G. Wu. *Appl. Phys. Lett.*, 2009, **94,** 144103.
14 S. Cheng, Z. G. Wu. *Lab Chip*, 2010, **10,** 3227-3234.
15 H. J. Kim, C. Son, B. Ziaie. *Appl. Phys. Lett.*, 2008, **92**.
16 M. Kubo, X. F. Li, C. Kim, M. Hashimoto, B. J. Wiley, D. Ham, G. M. Whitesides. *Adv. Mater.*, 2010, **22,** 2749-2752.
17 P. Tseng, C. Murray, D. Kim, D. Di Carlo. *Lab Chip*, 2014, **14,** 1491-1495.
18 S. H. Jeong, A. Hagman, K. Hjort, M. Jobs, J. Sundqvist, Z. G. Wu. *Lab Chip*, 2012, **12,** 4657-4664.
19 Y. Zheng, Z. Z. He, J. Yang, J. Liu. *Sci Rep*, 2014, **4,** 4588.
20 M. D. Dickey, R. C. Chiechi, R. J. Larsen, E. A. Weiss, D. A. Weitz, G. M. Whitesides. *Adv. Funct. Mater.*, 2008, **18,** 1097-1104.
21 S. Cheng, Z. Wu. *Lab Chip*, 2012, **12,** 2782-2791.
22 S. Lee, J. Ha, S. Jo, J. Choi, T. Song, W. Il Park, J. A. Rogers, U. Paik. *Npg Asia Materials*, 2013, **5,** e66.
23 R. Renaudot, V. Agache, Y. Fouillet, G. Laffite, E. Bisceglia, L. Jalabert, M. Kumemura, D. Collard, H. Fujita. *Lab Chip*, 2013, **13,** 4517-4524.
24 R. Safavieh, D. Juncker. *Lab Chip*, 2013, **13,** 4180-4189.

